

ศึกษาแบบจำลองรอยต่อพีเอ็นที่สถานะคงตัวหนึ่งมิติ ด้วยระเบียบวิธีไฟไนต์เอลิเมนต์

Studying steady state one-dimensional p-n junction using finite element method

อดินันท์ เจ๊ะซู (Adinan Jehsu)^{1*}
ทีปานิส ชาชิโย (Teepanis Chachiyo)¹

บทคัดย่อ

เราทำการสร้างโปรแกรมเพื่อทำการแก้สมการสารกึ่งตัวนำโดยใช้ระเบียบวิธีไฟไนต์เอลิเมนต์ซึ่งประกอบด้วย 3 สมการ ได้แก่ (i) สมการปัวซง (ii) สมการความต่อเนื่องของอิเล็กตรอน และ (iii) สมการความต่อเนื่องของโฮล โดยทำการแก้สมการเหล่านี้อย่างซ้ำๆ ด้วยวิธีของกัมเมลและระเบียบวิธีเชิงตัวเลขที่ใช้คือไฟไนต์เอลิเมนต์แบบกาลูร์กิน ในขณะที่ทำการหาผลเฉลย อัลกอริทึมจะให้ข้อมูลสำคัญที่เกี่ยวข้องกับสิ่งประดิษฐ์สารกึ่งตัวนำเช่น สนามไฟฟ้า ศักย์ไฟฟ้า และความหนาแน่นพาหะภายในสิ่งประดิษฐ์ นอกจากนี้ยังสามารถคำนวณหาลักษณะเฉพาะของกระแส-ศักย์ไฟฟ้า ในที่นี้เราทำการจำลองกรณีตัวอย่างคือไดโอดรอยต่อพีเอ็น ซึ่งผลลัพธ์ที่ได้จากการคำนวณสอดคล้องดีกับงานวิจัยที่ถูกตีพิมพ์ก่อนหน้านี้โดย De Mari

Abstract

We have implemented a computer program that solved semiconductor device equations using the finite element method. A set of three coupled equations, (i) Poisson's equation, (ii) electron continuity equation, and (iii) hole continuity equation were solved iteratively using Gummel's method. The numerical method used was based on the Galerkin finite element scheme. Upon finding the solutions, the algorithm provided us with important information relevant to semiconductor devices such as electric field, potential, and carrier concentration within the device. In addition, I-V characteristic for the semiconductor device could be calculated. We simulated a representative case: p-n junction diode. The results were in good agreement with previously published studies by De Mari.

คำสำคัญ: ระเบียบวิธีไฟไนต์เอลิเมนต์ รอยต่อพีเอ็น วิธีของกัมเมล

Keywords: finite element method, p-n junction, Gummel's method.

¹ Department of Physics, Faculty of Science, Khon Kaen University, Khon Kaen, 40002, Thailand

* Corresponding author, e-mail: a_jehsu@hotmail.com;

Introduction

Semiconductor device simulation is the study of semiconductor devices such as p-n junctions, as shown in Figure 1, using numerical techniques and a simplified model. In addition to providing useful information about the I-V characteristics which is pertinent to the analysis of the behavior of the devices in electronic circuits, semiconductor device simulation also gives detailed information about how electrical potential, electric field, and charge carrier densities are distributed inside the physical devices.

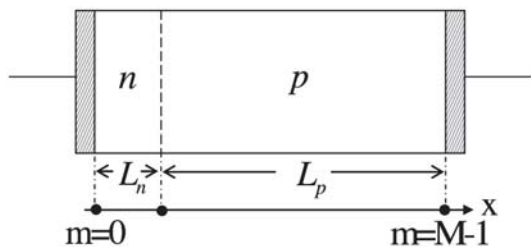


Figure 1. The p-n junction model in one dimension.

A typical theoretical modeling of semiconductor devices begins with five governing equations arising from five physical characters of the devices: 1) Poisson’s equation, 2-3) current densities of electrons and holes due to drift (electric field) and diffusion (concentration gradient), 4-5) continuity equations for electrons and holes.

In solving the system of equations, we need to resort to numerical methods in order to find the approximate solutions. Finite element is a numerical method of choice because it is suited for solving differential equations with complex geometries and boundary conditions. Even though the physical system we are pursuing as a case-study in this work, is merely a one-dimensional problem, initially implementing the finite element early on will provide us a firm ground for further development to 2 and 3

dimensional frameworks.

The purpose of this paper is to study the steady state one-dimensional p-n junction using the finite element method and compare our results with the results from De Mari. De Mari(1968) used the finite difference method and assumed (i) the absence of recombination in the interior of the device [$G(x) = 0$], (ii) an abrupt asymmetric impurity distribution, (iii) constant mobilities, and (iv) infinite recombination contacts (De Mari, 1968).

Theory and related words

Basic semiconductor device equations

A typical theoretical modeling of semiconductor devices begins with five governing equations. The explicit forms of these equations are given as follows, (Snowden, 1988).

$$\nabla^2 \psi = -\frac{q}{\epsilon}(C - n + p) \tag{1}$$

$$\bar{J}_n = -qn\mu_n \bar{\nabla} \psi + qD_n \bar{\nabla} n \tag{2}$$

$$\bar{J}_p = -qp\mu_p \bar{\nabla} \psi - qD_p \bar{\nabla} p \tag{3}$$

$$\bar{\nabla} \cdot \bar{J}_n - q \frac{\partial n}{\partial t} = qG \tag{4}$$

$$\bar{\nabla} \cdot \bar{J}_p + q \frac{\partial p}{\partial t} = -qG \tag{5}$$

Here, we briefly explain the notations used throughout this article.

- ψ electrostatic potential
- q electronic charge ($1.602 \times 10^{-19} \text{c}$)
- ϵ permittivity of the material which is equal to the product of the dielectric constant (ϵ_r) and the permittivity of free space ($\epsilon_0 = 8.854 \times 10^{-12} \text{F/m}$)
- C net impurity density which is equal to the difference between the donor impurity density (N_D) and the acceptor impurity density (N_A)

n	electron density
p	hole density
J_n	electron current density
J_p	hole current density
μ_n	electron mobility
μ_p	hole mobility
D_n	electron diffusion coefficient
D_p	hole diffusion coefficient
G	generation and recombination rate

Upon writing the five governing equations, instead of using the SI units, it is convenient to recast the physical quantities involved into ones whose units are dimensionless (De Mari, 1968). The normalization factors are listed in Table 1. The unit conversions have the key advantage that the physical quantities involved in the same equation have roughly the same order of magnitude, preventing the numerical problems which might occur due to round-off error when using a finite number of bits in the computer storage to represent a real number.

Table 1. List of normalization factors for the quantities of interest.

Description	Normalized quantity	Normalization factor
Position coordinate	x	$L_D = \sqrt{\epsilon_r \epsilon_0 V_t / q n_i}$
Electrostatic potential	ψ	$V_t = k_B T / q$
Applied voltage	V_A	V_t
Built-in potential	ϕ_{bi}	V_t
Intrinsic carrier density	n_i	n_i
Carrier densities	n, p	n_i
Net, donor, and acceptor impurity densities	C, N_D, N_A	n_i
Carrier diffusion coefficients	$\gamma_n^{-1}, \gamma_p^{-1}$	D_0 (equal to $1 \times 10^{-4} \text{ m}^2/\text{sec}$)
Carrier mobilities	$\gamma_n^{-1}, \gamma_p^{-1}$	D_0 / V_t
Total, electron, and hole current densities	J, J_n, J_p	$q D_0 n_i / L_D$

If we limit the scope of our study to a steady state in one-dimension, the five semiconductor device equations simplify to the following,

$$\frac{d^2}{dx^2} \psi(x) = n(x) - p(x) - C(x) \tag{6}$$

$$J_n(x) = \frac{1}{\gamma_n} \left[-n(x) \frac{d}{dx} \psi(x) + \frac{d}{dx} n(x) \right] \tag{7}$$

$$J_p(x) = \frac{1}{\gamma_p} \left[-p(x) \frac{d}{dx} \psi(x) - \frac{d}{dx} p(x) \right] \tag{8}$$

$$\frac{d}{dx} J_n(x) = G(x) \tag{9}$$

$$\frac{d}{dx} J_p(x) = -G(x) \tag{10}$$

The purpose of this study is to solve the system of non-linear coupled equations using the finite element method. However, in order to allow rigorous comparison between the numerical results given by De Mari (1968) which uses the finite different method and our calculations, we use the p-n junction with the exact same physical dimension and properties described in De Mari (1968) as our model. The physical parameters of the p-n junction are listed below.

Material: Germanium

$$\epsilon_r = 16, n_i = 2.5 \times 10^{19} \text{ m}^{-3}$$

Temperature: $T = 300 \text{ K}$

Doping:

n-side; $C(x) = N_D = 2.5 \times 10^{23} \text{ m}^{-3}$

p-side; $-C(x) = N_A = 2.5 \times 10^{21} \text{ m}^{-3}$

Length:

n-side; $L_n = 0.2 \times 10^{-6} \text{ m}$

p-side; $L_p = 1.4 \times 10^{-6} \text{ m}$ (for forward bias)

$L_p = 3.0 \times 10^{-6} \text{ m}$ (for reverse bias)

Carrier mobilities:

electron; $\mu_n = 3600 \times 10^{-4}, \frac{\text{m}^2}{\text{V} \cdot \text{sec}}$

hole; $\mu_p = 1700 \times 10^{-4} \frac{\text{m}^2}{\text{V} \cdot \text{sec}}$

Furthermore, in solving the differential equations, it is necessary to specify the boundary conditions. If we discretize the one dimension p-n junction into M nodes, with index ($m = 0$) signifying the first node, and the index ($m = M - 1$) denoting the last node as shown in Figure 1, these two nodes represent the boundary of the p-n junction model.

n-side:

$$\psi_0 = 0$$

$$n_0 = \frac{C_0 + \sqrt{C_0^2 + 4n_i^2}}{2}$$

$$p_0 = \frac{n_i^2}{n_0}$$

p-side:

$$\psi_{M-1} = V_A - \phi_{bi}$$

$$\phi_{bi} = \frac{k_B T}{q} \ln \left(\frac{p_{M-1}}{p_0} \right)$$

(ϕ_{bi} is the built-in potential)

$$n_{M-1} = \frac{C_{M-1} + \sqrt{C_{M-1}^2 + 4n_i^2}}{2}$$

$$p_{M-1} = \frac{n_i^2}{n_{M-1}}$$

where V_A potential is positive in the case of forward bias, and is negative in the case of reverse bias.

Computational details

Applying the Finite Element Method

We solve the system of equations using a finite element scheme, following the notation given by Reddy (1945). Here, we briefly describe to implementation; although the detailed methodology is provided in the original author's work (Reddy, 1945). The entire one dimensional model is divided into elements denoted by Ω_e , where x_a and x_b represent the beginning position and the ending position of each element accordingly. A set of many elements, called a mesh, forms the entire space of interest as shown in Figure 2.

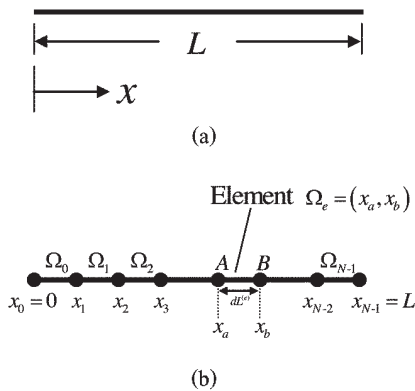


Figure 2. (a) Entire one dimensional model
(b) division into a set of elements

We begin by approximating the solutions, ψ , n and p in the e^{th} element according to

$$\tilde{\psi}^{(e)}(x) = \sum_{i=0}^{n-1} \psi_i^{(e)} L_i^{(e)}(x) \quad (11)$$

$$\tilde{n}^{(e)}(x) = \sum_{i=0}^{n-1} n_i^{(e)} L_i^{(e)}(x) \quad (12)$$

$$\tilde{p}^{(e)}(x) = \sum_{i=0}^{n-1} p_i^{(e)} L_i^{(e)}(x) \quad (13)$$

where n is the number of nodes within the elements; and the shape function $L_i^{(e)}(x)$ is defined by

$$L_i^{(e)}(x) = \sum_{k=0}^{n-1} a_{ki}^{(e)} x^k \quad i = 0, 1, \dots, n-1 \quad (14)$$

The set of coefficients a_{ki} are chosen in such a way that the shape function $L_i^{(e)}(x)$ assumes the value 1 at the i^{th} node while it vanishes at the other nodes. Hence, the coefficients a_{ki} can be determined using an inverse of the matrix shown.

$$[a]_{k \times i} = \begin{bmatrix} 1 & x_0 & x_0^2 & \dots & x_0^{n-1} \\ 1 & x_1 & x_1^2 & \dots & x_1^{n-1} \\ 1 & x_2 & x_2^2 & \dots & x_2^{n-1} \\ \vdots & \vdots & \vdots & \ddots & \vdots \\ 1 & x_{n-1} & x_{n-1}^2 & \dots & x_{n-1}^{n-1} \end{bmatrix}^{-1} \quad (15)$$

Then, instead of using the physical coordinate where each element begins at $x = x_a$ and ends at $x = x_b$, we perform a coordinate transformation into the so-called “natural coordinate” denoted by ξ where each element begins exactly at $\xi = -1$ and ends at $\xi = +1$.

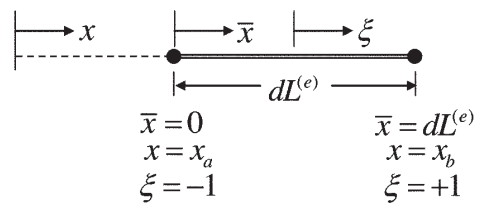


Figure 3. Boundary of each element in three different coordinate systems: global coordinate(x), local coordinate(\bar{x}), and natural coordinate(ξ).

The coordinate transformation from the global coordinate into the natural coordinate (i.e. $x = x_a \rightarrow \xi = -1$ and $x = x_b \rightarrow \xi = +1$) can be done by assuming a linear mapping equation,

$$x = a + b\xi \tag{16}$$

where a and b are constants that satisfy the transformation condition given previously.

In other words,

$$x_a = a + b(-1), \quad x_b = a + b(1) \tag{17}$$

Hence, a and b can be determined according to,

$$\begin{aligned} a &= \frac{1}{2}(x_b + x_a) = x_a + \frac{1}{2}dL^{(e)}, \\ b &= \frac{1}{2}(x_b - x_a) = \frac{1}{2}dL^{(e)} \end{aligned} \tag{18}$$

Substituting a and b into the mapping equation yields,

$$x(\xi) = x_a + \frac{1}{2}dL^{(e)}(1 + \xi) \tag{19}$$

Here x_a is the position where the element begins in global coordinate, and $dL^{(e)}$ is the length of the element. In a similar fashion as in Cartesian coordinate, the shape function can also be written in natural coordinates

$$L_i^{(e)}(\xi) = \sum_{k=0}^{n-1} a_{ki}^{(e)} \xi^k \tag{20}$$

with the usual properties

$$L_i^{(e)}(\xi_j) = \begin{cases} 1 & ; i = j \\ 0 & ; i \neq j \end{cases} \tag{21}$$

where ξ_j is the position of the j^{th} node in the element.

Table 2. Forms of the shape functions in natural coordinates.

Shape functions	The number of nodes in an element	node positions (left → right)
$L_i^{(e)}(\xi) = a_{0i}^{(e)} + a_{1i}^{(e)} \xi$	2	-1, 1
$L_i^{(e)}(\xi) = a_{0i}^{(e)} + a_{1i}^{(e)} \xi + a_{2i}^{(e)} \xi^2$	3	-1, 0, 1
$L_i^{(e)}(\xi) = a_{0i}^{(e)} + a_{1i}^{(e)} \xi + a_{2i}^{(e)} \xi^2 + a_{3i}^{(e)} \xi^3$	4	$-1, -\frac{1}{3}, \frac{1}{3}, 1$

Very often the finite element method requires an evaluation of the integration of a function $F(x)$ such as $\int_{x_a}^{x_b} F(x)dx$. In transforming to natural coordinate, the integration assumes much simpler limits of integration.

$$\begin{aligned} \int_{x_a}^{x_b} F(x)dx &= \int_{-1}^{+1} \hat{F}(\xi)d\xi, \\ \hat{F}(\xi)d\xi &= F(x(\xi))dx \end{aligned} \tag{22}$$

In addition, the small displacement d_x in the global coordinate is related to the infinitesimal displacement d_ξ in natural coordinates as follows

$$dx = \frac{dx}{d\xi} d\xi = J_e d\xi \tag{23}$$

where, J_e is called the Jacobian of the transformation; and it can be determined according to

$$J_e = \frac{dx}{d\xi} = \frac{d}{d\xi} \left(x_a + \frac{1}{2}dL^{(e)}(1 + \xi) \right) = \frac{1}{2}dL^{(e)} \tag{24}$$

Therefore, we have obtained a very useful mathematical identity for transforming an integral over a range $x_a \rightarrow x_b$ in the global coordinate into the natural coordinates as follows,

$$\int_{x_a}^{x_b} F(x)dx = \int_{-1}^{+1} F(x(\xi))J_e d\xi \tag{25}$$

Before we proceed directly to solve the set of semiconductor device equations given in Equation (6)- Equation(10), we need to rewrite Poisson’s equation into the form suggested by Gummel (1964). This mathematical technique is necessary for practical implementation because Poisson’s equation in its usual form often leads to very slowly converging calculation due to its non-linear character.

Consider a typical scheme for solving a non-linear coupled system of equations as shown in Figure 4. We begin by giving an initial guess of the electric potential $\{\psi_m^{(k)}\}$ at each node, so that the continuity equation for electron and hole can be initially solved, giving the approximate value for $\{n_m\}$ and $\{p_m\}$. These two pieces of information are used to repeat the entire cycle by solving Poisson equation, yielding again the electric potential $\{\psi_m^{(k+1)}\}$. The calculations are done iteratively until the electric potential $\{\psi_m^{(k+1)}\}$ converges to a final solution.

As mentioned previously, without proper treatment of Poisson’s equation using Gummel’s method (1964), the convergence becomes extremely slow. Here we briefly review Gummel’s method (1964) for the completeness of the discussion, but the detailed analysis will be omitted. Suppose the iterative cycle has proceeded to the k^{th} cycle, then the Poisson’s equation for the next cycle is typically of the form

$$\frac{d^2}{dx^2} \psi^{(k+1)} = n^{(k+1)} - p^{(k+1)} - C^{(k+1)} \quad (26)$$

Gummel suggested that the electric potential be written as

$$\psi^{(k+1)} = \psi^{(k)} + \delta\psi \quad (27)$$

The idea behind this scheme is that if the iteration is to be considered as already convergent, the deviation $\delta\psi$ has to diminish. If it is not yet converged however, then we need to find the value of $\delta\psi$ in order to find $\psi^{(k+1)}$. In a similar fashion for the electric potential, write,

$$n^{(k+1)} = n^{(k)} + \delta n \quad \text{and} \quad p^{(k+1)} = p^{(k)} + \delta p \quad (28)$$

The next step is to try to write δn and δp as function of $\delta\psi$, which Gummel suggested to be

$$\delta n = +n\delta\psi \quad \text{and} \quad \delta p = -p\delta\psi \quad (29)$$

Substituting Equation (27), (28), and (29) into Equation and canceling $\delta\psi$ from both sides of the equation yields

$$\begin{aligned} & \frac{d^2}{dx^2} \psi^{(k+1)} - (n^{(k)} + p^{(k)}) \psi^{(k+1)} \\ & = [n - p - C - \psi(n + p)]^{(k)} \end{aligned} \quad (30)$$

The above equation is essentially a Poisson equation, modified by Gummel so that it becomes suitable for solving iteratively. To avoid confusion, we will refer to Equation (30) as the “Modified Poisson’s Equation”.

1. Modified Poisson’s Equation

If the exact values for electric potential $\psi(x)$, the electron density $n(x)$, and the hole density $p(x)$ were known, both sides of the Equation (30) would be exactly equal. However, due to the approximate characters of these quantities, both sides are different by a certain amount, typically called the “Residual”. Define the residual R_1

$$\begin{aligned} & \frac{d^2}{dx^2} \tilde{\psi}^{(k+1)} - (\tilde{n}^{(k)} + \tilde{p}^{(k)}) \tilde{\psi}^{(k+1)} \\ & - [\tilde{n} - \tilde{p} - \tilde{C} - \tilde{\psi}(\tilde{n} + \tilde{p})]^{(k)} = R_1 \end{aligned} \quad (31)$$

where $\tilde{\psi}$, \tilde{n} , and \tilde{p} denote the approximate electric potential, electron density, and hole density accordingly. Realizing that the smaller the residual the more accurate the approximation becomes, the Galerkin finite element method demands that the integral over the entire domain of the residual

weighted by the shape functions must be zero. In other words,

$$\int_{\Omega_e} L_i^{(e)} R_1 dx = 0 \tag{32}$$

Substituting Equation (31) into Equation (32) yields

$$\int_{\Omega_e} L_i^{(e)} \left[\frac{d^2}{dx^2} \tilde{\psi}^{(k+1)} \right] dx - \int_{\Omega_e} L_i^{(e)} \left[(\tilde{n}^{(k)} + \tilde{p}^{(k)}) \tilde{\psi}^{(k+1)} \right] dx = \int_{\Omega_e} L_i^{(e)} \left[\tilde{n} - \tilde{p} - \tilde{C} - \tilde{\psi}(\tilde{n} + \tilde{p}) \right]^{(k)} dx \tag{33}$$

Consider the integration by parts of the first term on the left hand side

$$\int_{\Omega_e} L_i^{(e)} \left[\frac{d^2}{dx^2} \tilde{\psi}^{(k+1)} \right] dx = \left(L_i^{(e)} \frac{d}{dx} \tilde{\psi}^{(k+1)} \right) \Big|_{x_0}^{x_{n+1}} - \int_{\Omega_e} \frac{d}{dx} L_i^{(e)} \frac{d}{dx} \tilde{\psi}^{(k+1)} dx$$

As we impose the continuity condition of the electric field, $\left(-\frac{d}{dx} \tilde{\psi}(x_{n+1}) \right)^{(e)} = \left(-\frac{d}{dx} \tilde{\psi}(x_0) \right)^{(e+1)}$ and boundary condition, the first terms cancel, leaving the final result for the finite element equation as follows,

$$- \int_{\Omega_e} \frac{d}{dx} L_i^{(e)} \frac{d}{dx} \tilde{\psi}^{(k+1)} dx - \int_{\Omega_e} L_i^{(e)} \left[(\tilde{n}^{(k)} + \tilde{p}^{(k)}) \tilde{\psi}^{(k+1)} \right] dx = \int_{\Omega_e} L_i^{(e)} \left[\tilde{n} - \tilde{p} - \tilde{C} - \tilde{\psi}(\tilde{n} + \tilde{p}) \right]^{(k)} dx$$

The equations in the integral form must then be converted to a system of linear equations. Here, the i^{th} equation can be written as

$$\sum_{j=0}^{n-1} P_{ij}^{(e)} \psi_j^{(e, k+1)} = B_i^{(e)} \tag{35}$$

where
$$P_{ij}^{(e)} = - \int_{\Omega_e} \left[\left(\frac{d}{dx} L_i^{(e)} \right) \left(\frac{d}{dx} L_j^{(e)} \right) + L_i^{(e)} L_j^{(e)} (\tilde{n}^{(k)} + \tilde{p}^{(k)}) \right] dx$$

$$B_i^{(e)} = \int_{\Omega_e} L_i^{(e)} \left[\tilde{n} - \tilde{p} - \tilde{C} - \tilde{\psi}(\tilde{n} + \tilde{p}) \right]^{(k)} dx$$

2. Electron Continuity Equation

From Equation (9), we can define residual (R_2)

$$\frac{d}{dx} J_n - G = R_2 \tag{36}$$

According to the Galerkin finite element method, the integral over the entire domain of the residual weighted by the shape functions must vanish.

In other words,

$$\int_{\Omega_e} L_i^{(e)} \left[\frac{d}{dx} J_n - G \right] dx = 0 \tag{37}$$

The integrand contains two terms. Integrating

$$\int_{\Omega_e} L_i^{(e)} \frac{d}{dx} J_n dx \quad \text{by parts yields terms of the types}$$

$$(J_n(x_{n-1}))^{(e)} + (-J_n(x_0))^{(e+1)} \quad \text{which are}$$

guaranteed to vanish because of the continuity of the current density at the element boundary. Therefore, the finite element equation is

$$-\int_{\Omega_e} \frac{d}{dx} L_i^{(e)} J_n dx = \int_{\Omega_e} L_i^{(e)} G dx \quad (38)$$

Substituting the expression for electron current density from Equation (7) into Equation (38) gives

$$\int_{\Omega_e} \frac{d}{dx} L_i^{(e)} \left[\frac{1}{\gamma_n} \left(\tilde{n} \frac{d}{dx} \tilde{\psi} - \frac{d}{dx} \tilde{n} \right) \right] dx = \int_{\Omega_e} L_i^{(e)} \tilde{G} dx$$

which must be converted into a system of \mathbf{N} linear equations. Here, the i^{th} equation is given can be written as

$$\sum_{j=0}^{n-1} M_{ij}^{(e)} n_j^{(e)} = G_i^{(e)} \quad (39)$$

where

$$M_{ij}^{(e)} = \int_{\Omega_e} \frac{1}{\gamma_n} \left(\frac{d}{dx} L_i^{(e)} \right) \left[L_j^{(e)} \frac{d}{dx} \tilde{\psi} - \frac{d}{dx} L_j^{(e)} \right] dx$$

$$G_i^{(e)} = \int_{\Omega_e} L_i^{(e)} \tilde{G} dx$$

3. Hole Continuity Equation

In the same manner as the electron continuity equation, we can write the hole continuity equation into its Galerkin finite element form using Equation (10)

$$-\int_{\Omega_e} \frac{d}{dx} L_i^{(e)} J_p dx = -\int_{\Omega_e} L_i^{(e)} G dx \quad (40)$$

Substituting the hole current density in Equation (8) into Equation (40) gives

$$\int_{\Omega_e} \frac{d}{dx} L_i^{(e)} \left[\frac{1}{\gamma_p} \left(\tilde{p} \frac{d}{dx} \tilde{\psi} + \frac{d}{dx} \tilde{p} \right) \right] dx = -\int_{\Omega_e} L_i^{(e)} \tilde{G} dx \quad (41)$$

which must be converted into a system of \mathbf{N} linear equations. Here, the i^{th} equation can be written as

$$\sum_{j=0}^{n-1} Q_{ij}^{(e)} p_j^{(e)} = -G_i^{(e)} \quad (42)$$

where

$$Q_{ij}^{(e)} = \int_{\Omega_e} \frac{1}{\gamma_p} \left(\frac{d}{dx} L_i^{(e)} \right) \left[L_j^{(e)} \frac{d}{dx} \tilde{\psi} + \frac{d}{dx} L_j^{(e)} \right] dx$$

$$G_i^{(e)} = \int_{\Omega_e} L_i^{(e)} \tilde{G} dx$$

Finally, we have transformed the five governing equations into the Galerkin finite element scheme as shown in Equations(35), (39) and (42), which can be expressed in matrix form as follows,

$$[P^{(e)}] \{\psi^{(e)}\} = \{B^{(e)}\} \quad (43)$$

$$[M^{(e)}] \{n^{(e)}\} = \{G^{(e)}\} \quad (44)$$

$$[Q^{(e)}] \{p^{(e)}\} = -\{G^{(e)}\} \quad (45)$$

We then proceed to evaluate the elements of the matrices $[P^{(e)}]$, $[M^{(e)}]$, and $[Q^{(e)}]$, and the elements of the vectors $\{B^{(e)}\}$, and $\{G^{(e)}\}$ for every elements in the mesh. Solving the system of linear equations in matrix form as shown previously yields the electric potential $\{\psi^{(e)}\}$, electron density $[n^{(e)}]$, and hole density $[p^{(e)}]$ accordingly.

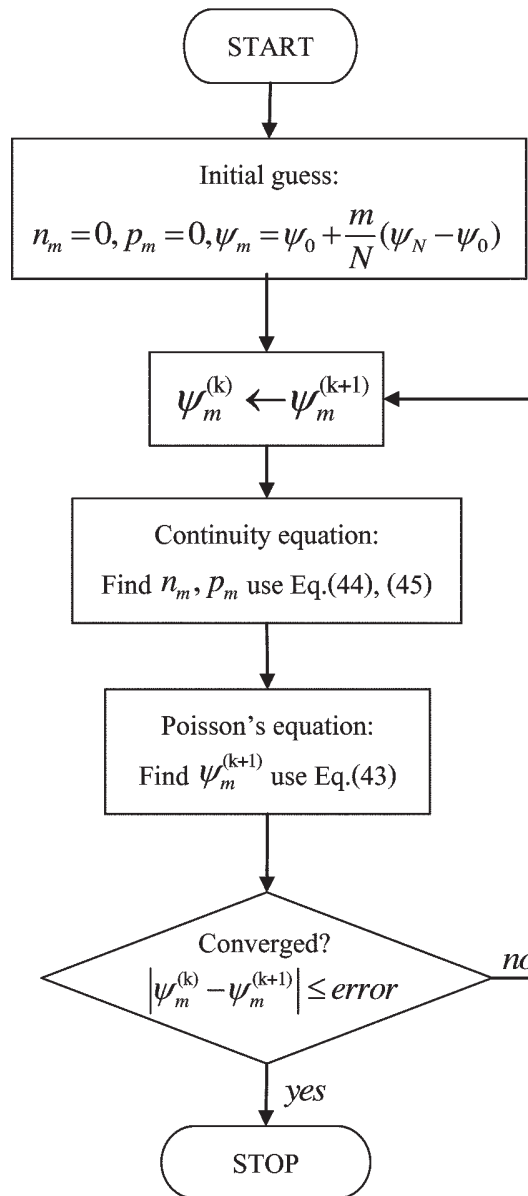


Figure 4. Flowchart of the calculation.

Results and discussion

In this work, we studied the p-n junction using the finite element method for three cases of applied voltage: 0, 4, and 22 (in normalized units). The computational methods explained previously were

implemented in C programming language. Specific parameters for each case such as the number of cycles, and maximum error of the electric potential as compared to the De Mari's (1968) result were listed in Table 3. In addition, we used the following parameters for all cases.

The number of elements = 600

The number of nodes in an element = 2

cut-off $|\psi_m^{(k)} - \psi_m^{(k+1)}|$ for convergence criteria = 1×10^{-6}

Figures 5, and 6 illustrates the case where no voltage is applied (no bias). Specifically, Figure 5 shows how the electric potential $\psi(x)$ distributes over the internal region of the device. Note the rapid increase of $\psi(x)$ near the interface between the n-type and the p-type, signifying the relatively larger electric field at the region. In the case where no bias is applied, the potential difference between both sides of the electrode is equal to the built-in potential given in Table 3. Figures 6(a) and 6(b) shows the charge carrier densities in linear scales and in semi-logarithmic scales respectively. Note how the electron accumulates in the n-type region, whereas the holes density is larger at the p-type region, consistent with widely accepted characteristics of a typical p-n junction diode.

Figures 7 and 8 are the calculated electric potential and charge carrier densities with the applied voltage equal to 4 in the dimensionless units. In addition, the results reported by De Mari (1968) are also plotted on the same graphs for comparison, showing satisfactory agreements.

Figures 9 and 10 are similar to the previous sets, except for the applied voltage being equal to 22 units. The comparisons with the De Mari (1968) results are also satisfactory in this case, giving much confident that our implementation using the finite element method is correct.

The agreement shown in these cases provides a solid ground when applying our implementation to study other p-n junction diodes or even a simple model for a one-dimensional transistor. In doing so, we only have to adjust the doping profile $C(x)$, the device dimensions, or boundary condition, while leaving the internal structure of the computational method unchanged (i.e. using the same computer program).

In addition to the electric potential $\psi(x)$, electron density $n(x)$, and hole density $p(x)$, I-V characteristics of a semiconductor device are also very useful information because the I-V curve of the device determines its behavior in electronic circuits. Figure 11 shows the current densities as a function of applied voltage which can be interpreted as the I-V characteristic of the p-n junction, where J denotes the total current density, and J_p is the hole current density.

Table 3. Numerical parameters for the three case studies.

Applied Voltage	Number of iterations	Max. error of potential	Difference potential
0	9	1.933E-008	13.816 (Built-in potential)
4	4	1.139E-007	9.816
22	34	7.468E-007	8.184

Conclusion

We have implemented a computer program that solves semiconductor device equations using the finite element method. A set of three coupled

equations: (i) Poisson's equation, (ii) electron continuity equation, and (iii) hole continuity equation; were solved iteratively using Gummel's method. The numerical method used was based on the Galerkin finite element scheme. Upon finding the solutions,

the algorithm provided us with important information relevant to semiconductor devices such as electric field, potential, and carrier concentration within the device. In addition, I-V characteristics for the semiconductor device could be calculated. We simulated a representative case: p-n junction diode. The results were in good agreement with previously published studies by De Mari.

References

- De Mari, A. 1968. An accurate numerical steady-state one-dimensional solution of the p-n junction. **Solid State Electronics** 11(1): 33-58.
- Reddy, J. N. 1945. **An introduction to the finite element method**. 3rd ed. New York: McGraw-Hill.
- Gummel, H.K. 1964. A self-consistent iterative scheme for one-dimensional steady state transistor calculations. **IEEE Transactions on Electron Devices** 11: 455-460.
- Snowden, C. M. 1988. **Semiconductor device modeling**. London: Shot Run Press Ltd.

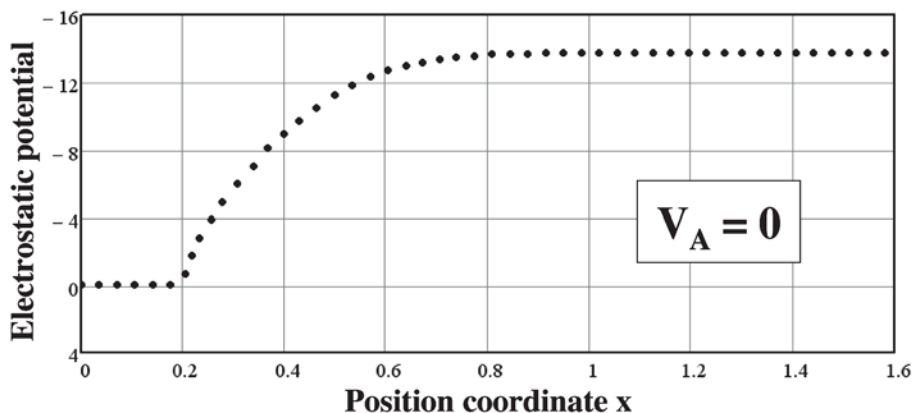


Figure 5. Electrostatic potential as a function of position in no-bias case.

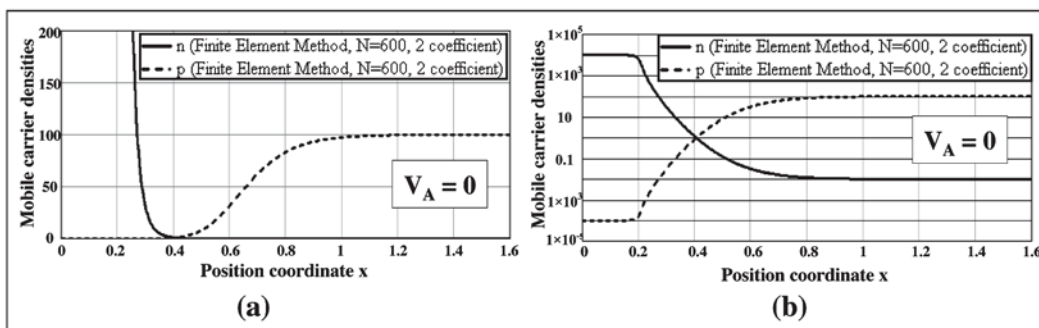


Figure 6. Mobile carrier densities as function of position in no-bias case (a) linear scales (b) semilogarithmic scales.

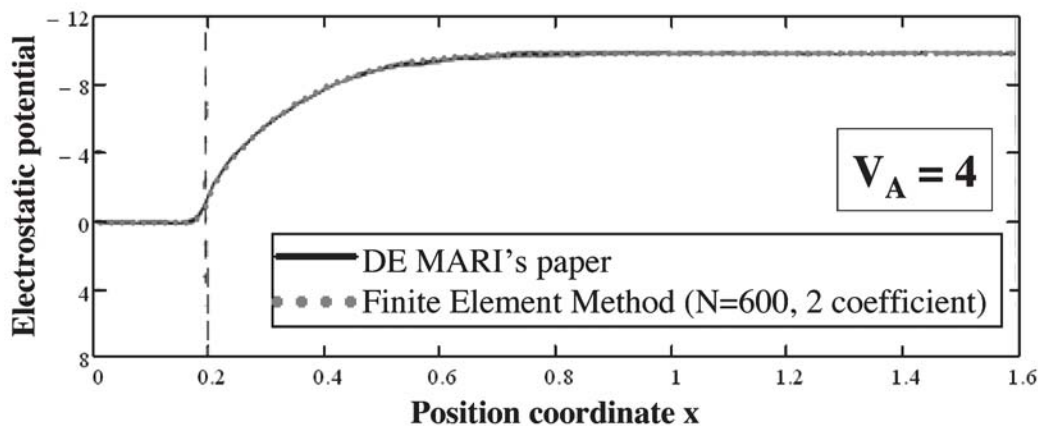


Figure 7. Comparison between the electric potential $\psi(x)$ in this work (dotted-line) and in De Mari's work (solid-line).

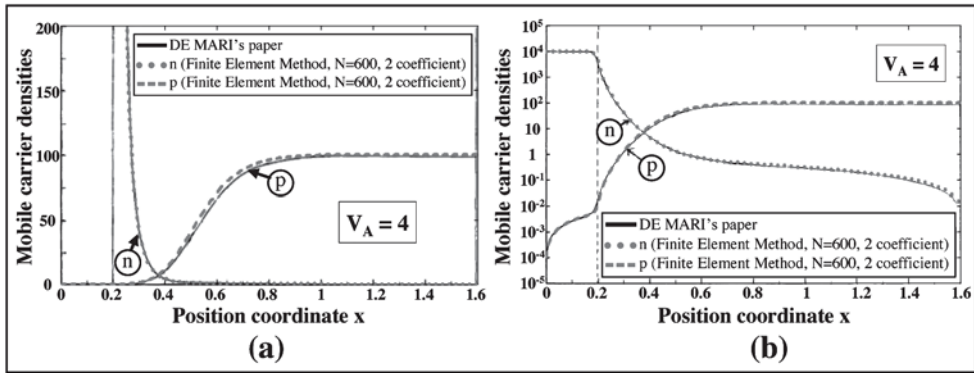


Figure 8. Mobile carrier densities as functions of position when applied voltage is 4 (in dimensionless units)
 (a) linear scales (b) semi-logarithmic scales.

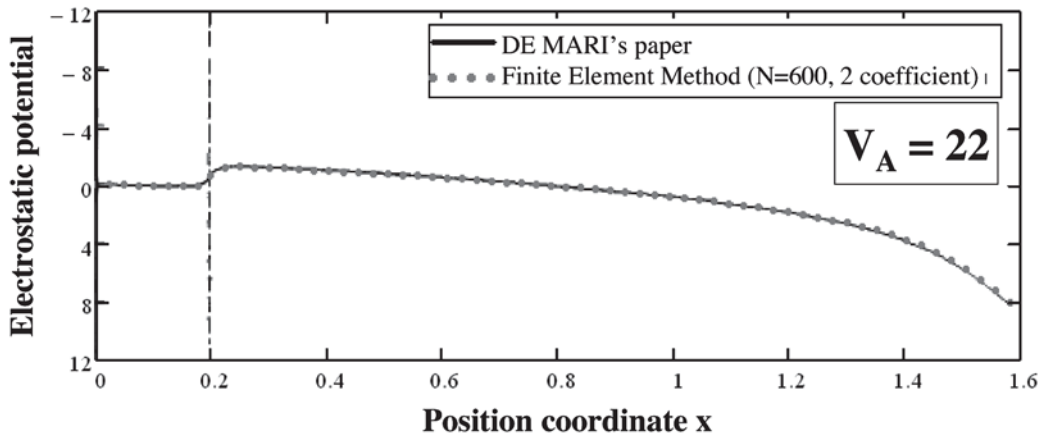


Figure 9. Electric potential $\psi(x)$ under 22 (in dimensionless units) applied voltage.

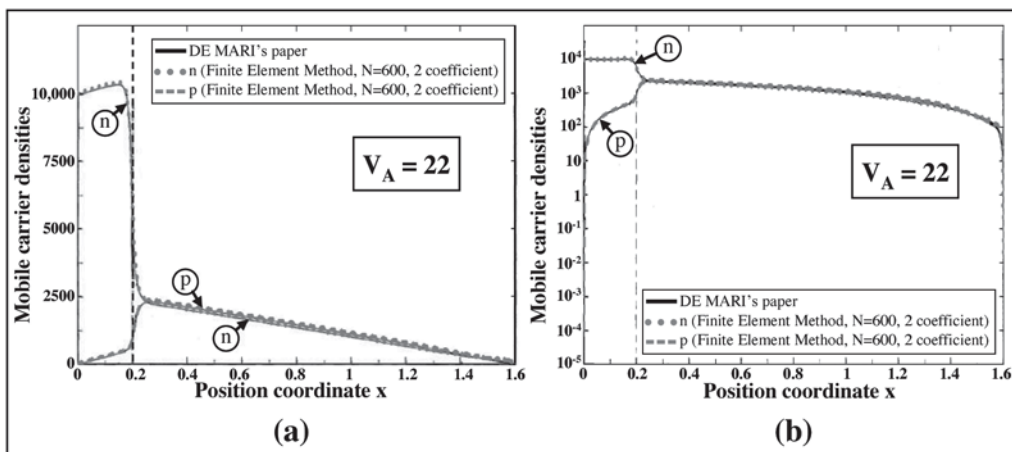


Figure 10. Electron density and hole density under 22 applied voltage (a) linear scales (b) semi-logarithmic scales.

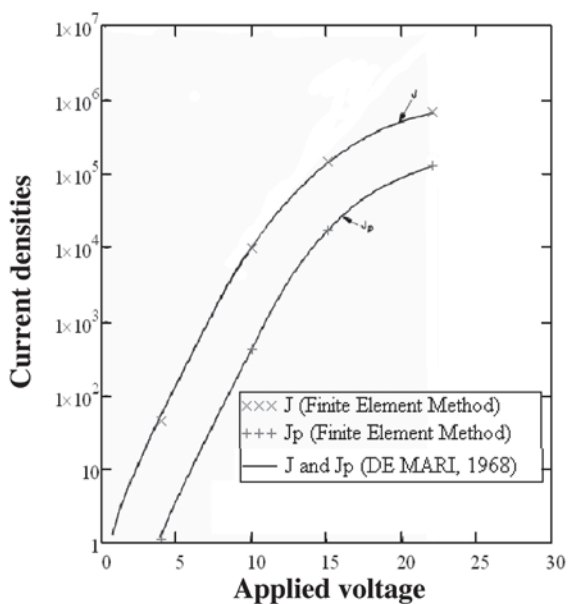


Figure 11. Current densities as a function of applied voltage. J denotes the total current density and J_p is the hole current density.